24/01/2025 05:42

(Article begins on next page)

Does subduction of mass transport deposits (MTDs) control seismic behavior of shallow–level megathrusts at convergent margins?

(Article begins on next page)

16 February 2022

UNIVERSITA' DEGLI STUDI DI TORINO

Does subduction of mass transport deposits (MTDs) control seismic behavior of shallow–level megathrusts at convergent margins?

Andrea Festa [a,*], Yildirim Dilek [b], Silvia Mittempergher [c], Kei Ogata [d], Gian Andrea Pini [e], Francesca Remitti [f]

[a] Dipartimento di Scienze della Terra, Università di Torino, Torino, Italy
[b] Department of Geology and Environmental Earth Science, Miami University, Oxford, OH, USA
[c] Dipartimento di Scienze dell'Ambiente e della Terra, Università di Milano Bicocca, Milano, Italy
[d] Faculty of Science, Vrije Universiteit, Amsterdam, The Netherlands
[e] Dipartimento di Matematica e Geoscienze, Università di Trieste, Trieste, Italy
[f] Dipartimento di Scienze Chimiche e Geologiche, Università di Modena e Reggio Emilia, Modena, Italy

Abstract

We present a critical appraisal of the role of subducted, medium (10–$1000\ km^2$) to giant ($\geq 1000\ km^2$) and het- erogeneous, mud-rich mass transport deposits (MTDs) in seismic behavior and mechanisms of shallow earth- quakes along subduction plate interfaces (or subduction channels) at convergent margins. Our observations from exhumed ancient subduction complexes around the world show that incorporation of mud-rich MTDs with a "chaotic" internal fabric (i.e., sedimentary mélanges or olistostromes) into subduction zones strongly modifies the structural architecture of a subduction plate interface and the physical properties of subducted ma- terial. The size and distribution of subducted MTDs with respect to the thickness of a subduction plate interface are critical factors influencing seismic behavior at convergent margins. Heterogeneous fabric and compositions of subducted MTDs may diminish the effectiveness of seismic ruptures considerably through the redistribution of overpressured fluids and accumulated strain. This phenomenon possibly favors the slow end-member of the spectrum of fault slip behavior (e.g., Slow Slip Events, Very Low Frequency Earthquakes, Non-Volcanic Tremors, creeping) compared to regular earthquakes, particularly in the shallow parts (T b 250 °C) of a subduction plate interface.

1. Introduction

Most large magnitude earthquakes (Mw ≥ 8.5) that occurred in the past are shown to have taken place along the frictional interface be- tween two converging plates at subduction zones (e.g., Byrne et al., 1988; Scholz, 2002; Heuret et al., 2012; Scholl et al., 2015). Several interlinked geological, physical and mechanical factors have been pro- posed to explain different seismic behaviors of subduction plate inter- face, such as the coupling strength (e.g., Lay and Kanamori, 1981; see also Uyeda and Kanamori, 1979; Scholz and Campos, 2012; Doglioni et al., 2007), slab retreat (e.g., Doglioni et al., 2007), upper plate motion and the related-stress regime (Peterson and Seno, 1984; Scholz and Campos, 1995; Heuret et al., 2012), down-dip width of a seismogenic zone (e.g., Kelleher et al., 1974; Corbi et al., 2017), megathrust curvature (Bletery et al., 2016), and trench migration velocity (Schellart and Rawlinson, 2013). Among these factors, subduction of thick piles of trench sediments (i.e., thickness ≥ 1 km) appears to play a critical role in facilitating seismic rupture propagation and high-magnitude

earthquake occurrences (Mw ≥ 8.5), by smoothing out lateral relief gradient and strength-coupling asperities at a subduction plate interface (Ruff, 1989; Heuret et al., 2012; Scholl et al., 2015; Seno, 2017; Brizzi et al., 2018). However, the occurrence of giant earthquakes (Fig. 1) at convergent plate boundaries, which are characterized by both sediment-flooded (e.g., Sumatra, Central-South Chile, Alaska/Aleutians) and sediment-poor trenches (e.g., Kamchatka, Northern Chile, Northern Peru, Northern Japan) (see, e.g., Kopp, 2013), suggests that some other factors such as the internal architecture and the mechanical properties of subducted material (e.g., composition, friction and strength proper- ties, permeability, stiffness, fracture toughness; Fagereng and Sibson, 2010 and reference therein), as well as the thickness of a subduction plate interface (Rowe et al., 2013), may play a more significant role than sediment supply rates in influencing the seismic behavior at shal- low depths in subduction zones. Particularly, subduction of heteroge- neous material characterized by strong internal contrast in competence that is typical of mélanges and shear zones has been re- ported as a significant factor affecting seismic style within a subduction plate interface or in a subduction channel shear zone (e.g., Cloos, 1982; Raymond, 1984; Cowan, 1985; Festa et al., 2010; Codegone et al., 2012; Dilek et al., 2012). Mixing of competent blocks of oceanic crust with
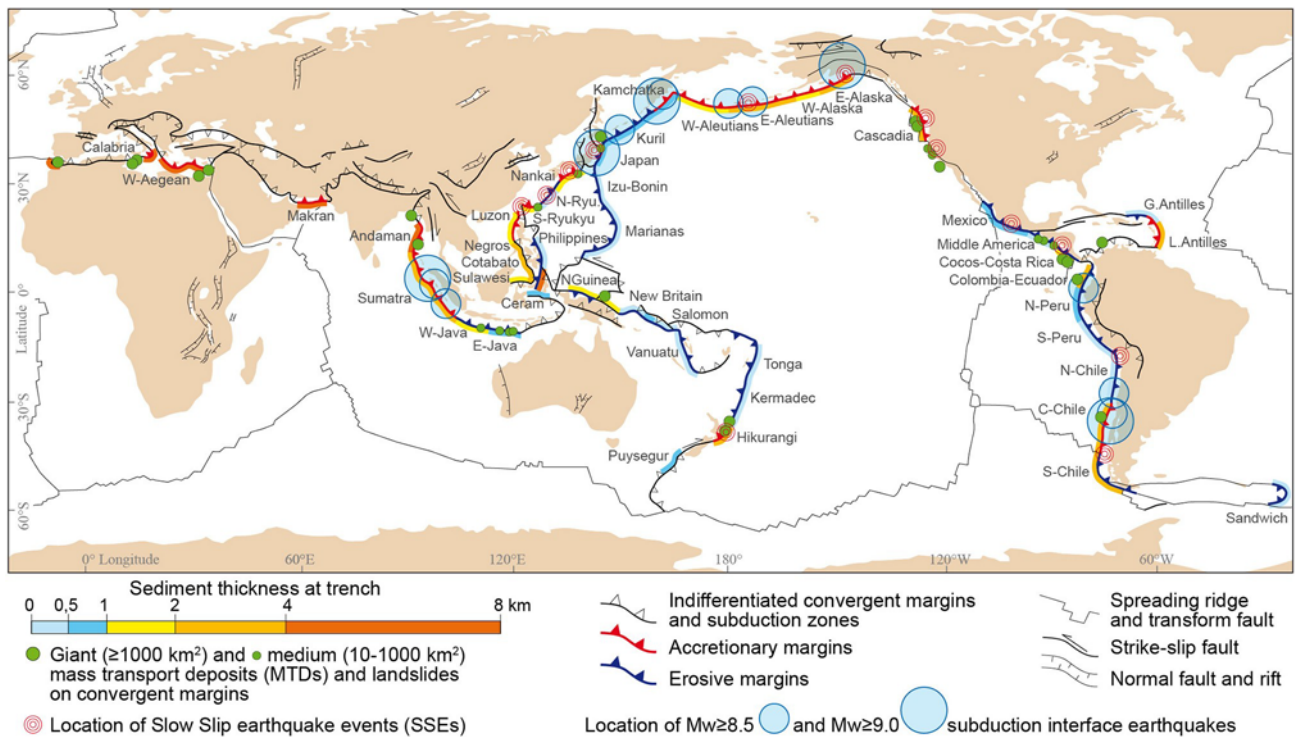
Fig. 1. Global distribution of accretional and erosional subduction zones (modified from Clift and Vannucchi, 2004; Scholl and von Huene, 2009) and the distribution of subduction interface earthquakes with magnitudes N8.5 (from Heuret et al., 2012; Scholl et al., 2015). The color bar shows sediment thickness variations in different trenches (modified from Clift and Vannucchi, 2004; Heuret et al., 2012; Scholl et al., 2015). Also shown on this map are slow slip earthquake events (SSEs; from Obara and Kato, 2016), and medium (area 10–1000 km²) to giant (area N 1000 km²) mass transport deposits (from von Huene et al., 2004; Urgeles and Camerlenghi, 2013; Festa et al., 2016; Moscardelli and Woods, 2016).

incompetent fluid-saturated trench-fill sediments and big differences in the proportion between competent blocks and weak matrix material create the highest competence gradient (Fagereng and Sibson, 2010).

Complex interplay between all these geological, physical and mechanical factors constitutes a major cause for a wide range of slip behaviors observed at a large number of subduction plate interfaces around the world. Slip rates may range from plate convergence rates (1–10 cm·year^{-1}) during aseismic creep to slip rates of ~1 m·s^{-1} during earthquake propagation (e.g., Fagereng and den Hartog, 2016 and reference therein). In between these end members, different types of slow-slip events (SSEs) and low-frequency earthquakes (LFEs) show an intermediate range of slip rates with durations of days or years, representing a transitional seismic state between stable sliding (i.e., steady aseismic creep) and earthquake rupturing (e.g., Ide et al., 2007; Schwartz and Rokosky, 2007; Peng and Gomberg, 2010; Obara and Kato, 2016).

In this paper, we examine heterogeneous, mud-rich mass transport deposits (MTDs hereafter) subducted along subduction plate interfaces, and discuss how they may affect the seismic behavior at convergent margins by strongly modifying the internal architecture and the mechanical – physical properties of subducted material. We suggest that the heterogeneous fabric and compositions of subducted MTDs may diminish the effectiveness of seismic ruptures, favoring mixed continuous-discontinuous shearing. Because it is highly difficult to decipher the internal architecture and composition of modern subduction plate interfaces through seismic reflection and tomography studies, our observations and interpretations presented here are largely based on on–land analogues of megathrust shear zones in ancient subduction complexes exposed in the Northern Apennines (Italy), the peri–Mediterranean region, the Appalachians, and the circum–Pacific region where the existence of fossil submarine MTDs is well documented. These exhumed, ancient MTDs show strong similarities in size, distribution, recurrence interval, and run-out distance with modern submarine slide deposits in active continental margins (e.g., Camerlenghi and Pini, 2009; Urgeles and Camerlenghi, 2013; Ogata et al., 2014a, 2014b; Festa et al., 2014, 2016; Moscardelli and Woods, 2016).

2. Temporal and spatial recurrence of MTDs in subduction-accretion complexes

MTDs represent earth material that has been redeposited on the seafloor following its remobilization and transportation as a result of slope failure, gravitational deformation and/or tectonic activities (Lamarche et al., 2008, and references therein). Although submarine MTDs may develop in various tectonic settings, they commonly occur on continental slopes at convergent margins where high fluid pressures, high-magnitude seismic events, high sedimentation rates, rapid crustal uplift, tectonic erosion, and swift critical taper adjustments contribute to slope instability (Coleman and Prior, 1988; McAdoo et al., 2000; Collot et al., 2001). These chaotic deposits are, therefore, significant components of subduction complexes. In this section, we first discuss the occurrence and distribution of MTDs in both modern and ancient subduction complexes, and then examine the fate of subducted MTDs.

2.1. Modern subduction-accretion complexes

High-resolution multibeam echosounding surveys (e.g., von Huene et al., 1989, 2004) at modern convergent margins have helped documenting a wide spectrum of MTDs (Fig. 1), ranging from slumps to slides (e.g., Japan Trough, see Strasser et al., 2013 and reference therein) and debris-blocky flows (e.g., the Ruatoria MTD in Hikurangi margin, see Collot et al., 2001) with km-size megablocks embedded in a mud-rich to debrite matrix (see also, e.g., Moscardelli and Woods, 2008; Geersen et al., 2011; Urgeles and Camerlenghi, 2013; Ogata et al., 2014a; Ortiz-Karpf et al., 2016). Medium (10–1000 km²) to giant (≥1000 km²) MTDs that are composed mainly of debris-blocky flows occur in both erosional and accretionary convergent margins (Figs. 1, 2A), independently of the thickness of trench-fill sediments
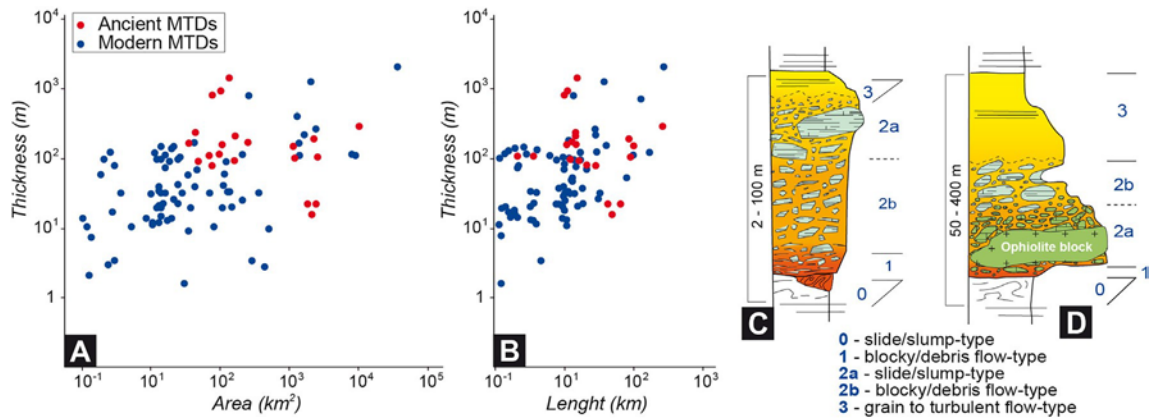
Fig. 2. (A) Logarithmic plots of average thickness versus average area, and (B) average thickness versus average length of modern and ancient MTDs observed in subduction complexes and convergent margins (data from from Woodcock, 1979; Ogata et al., 2014a; Festa et al., 2016; Moscardelli and Woods, 2016). Conceptual stratigraphic columnar sections (C and D), summarizing the end member types of ancient MTDs studied in the Northern Apennines (Italy). Recurrent structural facies associations are numbered from the base to the top (modified from Festa et al., 2016).

and the volumes and elevations of their accretionary and erosional wedges. Such MTDs are commonly located far from the epicenters of great (Mw ≥ 8.5) megathrust earthquakes, but are situated close to those sections of subduction plate interfaces in which SSEs, tremors and low- to very low-frequency earthquakes have been detected (Fig. 1). These types of large-scale MTDs may reach up to several 100-km-long run-out distances (Fig. 2B; see Urgeles and Camerlenghi, 2013; Moscardelli and Woods, 2016), and may emplace sedimentary material in excess of several tens of cubic-km along-strike of a trench. Some of the best examples of such MTD-derived, trench-fill sediment occurrences have been observed along the Hikurangi convergent margin of the North Island of New Zealand (Collot et al., 2001; Lewis et al., 2004; Ogata et al., 2014a), northern Peru Trench, (von Huene et al., 1989), Middle America Trench (Von Huene et al., 2004), Ecuador Trench (see Ratzov et al., 2010), the northern part of the central Chile Trench (Geersen et al., 2011), and Japan Trough (Strasser et al., 2013). The discrepancy between the volumes of some of those MTDs preserved in a trench compared with those in a slope embayment indicates that some submarine slide masses may locally have been incorporated into a subduction complex. For example, Geersen et al. (2013) have shown that the volume of two heterogeneous MTDs (~248 km^3 and ~127 km^3), which were incorporated into the subduction plate interface along the margin of Southern Chile, does not even match the estimated minimum volume (~472 km^3) of slope deposits, sourced from a 30 × 70 × 2 km topographic slope embayment and preserved in the trench.

The recurrence time for major episodes of MTD emplacement commonly ranges between 1 and 15 kyrs and ~100 kyrs (e.g., Ratzov et al., 2010; Geersen et al., 2011; Moscardelli and Woods, 2016; Ortiz-Karpf et al., 2016). An extrapolated power-law curve for MTDs documented from both passive and active continental margins in the Mediterranean Sea region indicates that only one slope failure in excess of 10 km^3 may happen every ~1000 years, whereas giant failures exceeding 10^3 km^3 are likely to occur at recurrence rates close to 40 kyrs (Urgeles and Camerlenghi, 2013). However, 1 or 2 small-scale slope failures (N10^{-3} km^3) are likely to occur every year (Urgeles and Camerlenghi, 2013).

2.2. Ancient subduction-accretion complexes

Ancient MTDs in exhumed subduction complexes commonly consist of highly heterogeneous rock assemblages (e.g., Mutti et al., 2006, and reference therein), produced by a wide spectrum of mass transport processes and composed of multiple sub-units (e.g., Lucente and Pini, 2003). These sub-units are comparable in size to their counterparts in modern submarine settings (Fig. 2A, B), and display inhomogeneous internal structures that are significantly affected by the degree of

lithification – consolidation of the source unit, and by the degree of internal disaggregation, run-out distance and mechanisms of downslope mobilization.

In this study, we mainly focus on mud-rich chaotic deposits (Type 1 MTDs of Pini et al., 2012), which represent one of the most common types of MTDs in modern subduction complexes (see, e.g., Pini et al., 2012; Festa et al., 2016; Moscardelli and Woods, 2016). These mud-rich MTDs consist of block-in-matrix deposits, such as sedimentary mélanges or olistostromes (Fig. 2C, D), which are characterized by cm- to m-sized lithic blocks made of limestone, marl, sandstone, siltstone and/or ophiolite units, that are randomly distributed in a clay- or shale-rich matrix. This weak matrix material behaves in a visco-plastic manner and generally exhibits a brecciated or clastic texture. It may sustain bedding packages locally reaching tens of meters or up to kilometers in size (floaters or over-sized blocks; Fig. 2C, D). Internally, this type of MTD consists of stacked up, different cohesive debris flow units, which range in thickness from meters to tens of meters, with each single debris flow deposit characterized by inverse grading of the largest blocks. At the base, an MTD is commonly bounded by a horizon of several dm-thick and sheared, argillaceous breccia with a matrix showing fluidal structures and spaced scaly fabric textures. This breccia makes a low-angle, sheared contact with the base of the MTD deposit (e.g., Pini, 1999; Festa et al., 2013, 2015). Field observations suggest that this type of MTDs may run relatively fast and for long distances (tens of kilometers; Fig. 2B; Pini, 1999; Pini et al., 2012; Festa et al., 2015, 2016), if aided by the physiography of the depositional setting and if underlain by an overpressured "carpet" of earth material consisting of a mixture of water and loose sediments (hydroplaning, Mohrig et al., 1998).

3. Subduction of MTDs and redistribution of deformation

Studies of fossil analogues of modern subduction complexes have shown that lithotypes and lithification degrees of different earth material within inter-plate shear zones strongly influence strain partitioning and distribution of shallow crustal deformation (e.g. Fisher and Byrne, 1987; Vannucchi et al., 2008, 2012; Dielforder et al., 2016). In a shallow part of a shear zone along a subduction zone plate interface (~40 °C–80 °C) strain localization occurs in a relatively weak material (i.e., clay rich and incompletely lithified components), resulting in pervasive deformation. As the lithification process continues and becomes completed (at temperatures around 120 °C–150 °C), rheological differences between subducted sediments with different compositions or textures become less important. This transition to a generally homogeneous rheology is marked by the development of thin faults marked by cm- to 100-m-long shear veins. These brittle structures form in all subducted

sediments in the presence of cyclic, high fluid pressures, which they crosscut (Kimura et al., 2012; Vannucchi et al., 2008). Thus, despite their diverse internal fabric, diagenetic path and lithification state, the mechanical behavior of subducted MTDs likely represents relative homogeneity compared to the surrounding trench sediments in the shallowest portions of a subduction plate interface shear-zone.

Mud-rich MTDs are typically less porous and more compacted than the surrounding trench sediments (e.g., Cardona et al., 2016). Detailed stratigraphic logs of some of MTDs with a block-in-matrix texture indicate that their sediments have greater bulk density, resistivity, and shear strength than undisturbed or slumped, bedded clays (Sawyer et al., 2009). These petrophysical properties likely derive from rearrangement and deformation of mud/clay-rich sediments during their down-slope mobilization. Experimental studies demonstrate that the remolded material consolidates to a lower porosity and higher density state in comparison to natural samples under an equivalent uniaxial stress conditions (e.g., Skempton, 1970). Occurrence of a shear-induced fabric in clayey material that may have developed during long runout distance transport may further reduce porosity and pore throat size (Cardona et al., 2016).

Given their relatively higher stiffness compared to their unlithified muddy host sediments, most MTDs commonly preserve their primary chaotic block-in-matrix fabric (Fig. 3A-C) during subduction at very shallow depths. This phenomenon suggests that subducting MTDs are not the site of preferential deformation. At depths corresponding to T ~60 °C-80 °C (~2 to ~3 km of vertical burial) along a plate subduction interface, weak flattening of both the matrix and soft blocks and clasts may occur (see Fig. 3A, D-E). Clasts of tabular to elongated, competent rocks and fragments of lithified layers may be preferentially aligned along the plane of flattening, whereas rounded to irregularly shaped clasts and fragments are randomly oriented within the matrix (Fig. 3E). These differences suggest volumetric deformation typical of incompletely lithified rocks. Some MTDs, which have been exhumed from burial depths along subduction plate interface, corresponding to T~80 °C-120 °C (~3 to ~4 km), display injection dikes and hydrofractures developed between competent blocks/clasts and a partially consolidated matrix (Fig. 3D). These features point to overpressure conditions and inhomogeneous fluid migration. In contrast, host sediments exhumed from burial depths of ~4 to ~5 km (corresponding to ~120 °C - 150 °C temperatures) are crosscut by well-developed slip surfaces (Fig. 3F), favoring compartmentalization and concentration of fluid pressures (Fig. 3G). These features indicate that sediments had relatively homogeneous shear strength, and that they were well lithified, with volume reduction up to 50% (e.g., Vannucchi et al., 2012) The
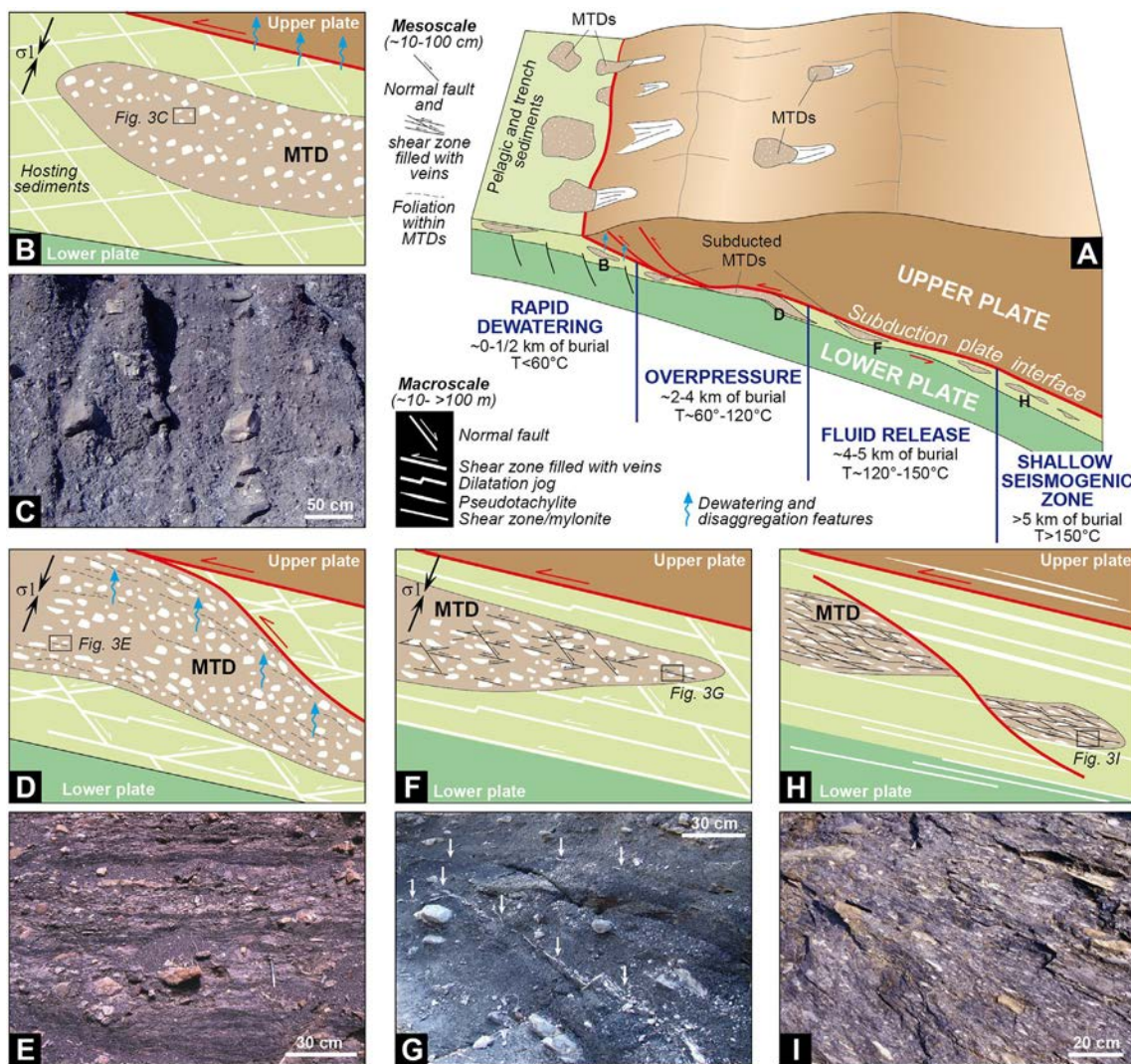
Fig. 3. (A) Conceptual model based on combined geophysical and geological observations from modern and ancient subduction – accretion complexes depicting MTDs with variable sizes (from small- to giant) situated within a subduction plate interface (modified from Vannucchi et al., 2012). (B through I) Interpretive diagrams and field photographs from the Northern Apennines (Italy), showing some of the characteristic features of four main zones of a subduction plate interface in a frontal thrust zone (B and C), in the up-dip limit of a shallow seismogenic zone (H and I). Details of the structural architecture of host sediments are modified from Vannucchi et al. (2012); internal fabric of MTDs are based on our field observations.

first appearance of brittle behavior in lithified components of subducted sediments was probably recorded at shallow conditions, around 80 °C (Fisher and Byrne, 1987; Dielforder et al., 2016; Mittempergher et al., 2017). This inference implies that even if the MTDs are initially relatively stiffer and less prone to deformation, their low permeability, isotropic nature and small volume reduction may slow down the lithification process with respect to host sediments, and may allow vast amounts of fluids to reach deeper down at subduction plate interfaces, strongly influencing strain partitioning both inside and along the boundaries of MTDs.

At depths corresponding to T N 150 °C (N~5 km of vertical burial) significant volume reduction occurs in MTDs, causing strong asymmetrical flattening and pervasive extensional shearing (Fig. 3I). Competent blocks and clasts become strongly elongated, showing phacoidal shape fabric, pinch-and-swell and symmetrical‑asymmetrical boudinage structures (Fig. 3H, I), extensional veining and shearing, and brecciation of tails and necks of blocks and pressure shadows (e.g., Pini et al., 2012; Platt, 2015; Festa et al., 2016). The mean size of blocks and clasts at these depths is commonly smaller than that observed at shallower structural levels. The matrix material in MTDs displays a pervasive scaly fabric and Riedel shears, which are commonly bounding competent blocks and clasts. Deformation is thus distributed along cm- to m-long discontinuities (e.g., micro-cracks; Fig. 3H), defining a "structurally ordered" block-in-matrix fabric (Fig. 3I), which closely resembles the main fabric observed in tectonically produced mélanges and broken formations on land (e.g., Cowan, 1985; Pini, 1999; Fagereng et al., 2011; Festa et al., 2013). Locally, tectonic slip may concentrate along the boundaries between MTDs and host sediments, and may overprint primary shear surfaces formed during gravitational emplacement.

4. Seismic behavior within subduction plate interface

The structural architecture and thickness of a subduction plate interface, the mechanical properties of subducted material, and the mode of the distribution of fluid overpressure constitute some of the critical factors controlling the seismic behavior at shallow depths at convergent margins (e.g., Fagereng and Sibson, 2010; Rowe et al., 2013). Subduction of mud-rich MTDs with a heterogeneous block-in-matrix fabric plays a significant role in modifying all these factors and hence exerts a major control on the nature of the seismic behavior along a subduction plate interface. The internal fabric and the 3D size of subducted MTDs with respect to the thickness of a subduction plate interface are the two most important characteristics of MTDs that affect the seismic behavior along subduction plate interfaces.

4.1. Internal fabric of MTDs and seismic behavior

At shallow structural levels along a subduction plate interface (~1/4 km of vertical burial, and T~60°‑120 °C), the role of the heterogeneous internal fabric of MTDs in controlling the relationships between fluid distribution and slip propagation is enhanced by the stronger contrast in the rheological and mechanical properties (e.g., lithification, compaction, permeability, porosity) with respect to those of host sediments. The less permeable and more compacted nature of subducted MTDs, in comparison to those of host sediments, acts as a significant barrier for fluid circulation, causing the concentration of shear in the more lithified and drier host sediments or at their boundary with MTDs (Fig. 3A-D). With increasing depths (T~120°‑150 °C), MTDs display slower lithification rates and behave rheologically differently in comparison to the surrounding sediments, especially in expelling water. These features increase the structural heterogeneity within the up-dip limit of a subduction plate interface, favoring the formation of a complex network of slip-surfaces with different lengths. They also cause strain localization along the boundaries of MTDs where fluid overpressure and weak mechanical surface response concentrate (Fig. 3F, G).

When MTDs completely lithify (T N 150 °C), their internal fabric becomes comparable to that of tectonic mélanges and broken formations (Figs. 3H‑I, 4B). The "structurally-ordered" block-in-matrix fabric of fluid-rich MTDs favors slow dispersion of high- to over-pressured fluids in a complex network of minor slip surfaces, and results in distribution of strain along several discrete anastomosing shear surfaces (Figs. 3H‑I, 4B), cm- to m-long, that wrap around competent blocks. The mixture of clay-rich (incompetent) matrix and competent blocks exhibits both discrete and distributed deformation with minimum interaction between adjacent blocks. This scenario creates unstable sliding material enclosed by frictionally stable sliding or conditionally stable matrix, similar to that proposed for tectonic mélanges (Fagereng and Sibson, 2010; Fagereng, 2011). Large ruptures may not nucleate, but development of several single-micro slip surfaces can trigger a particular type of highly repetitive slip with micro-displacements, causing microseismicity or a slip type that is transitional between stable sliding (i.e., steady aseismic creep) and fast rupture (i.e., stick-slip behavior). The relative slowness of LFEs and tremors (weeks to years; see Peng and Gomberg, 2010; Ito et al., 2013) that is widely detected along the circum-Pacific subduction zones (e.g., Ide et al., 2007; Schwartz and Rokosky, 2007; Peng and Gomberg, 2010; Obara and Kato, 2016), has been attributed to unusual material properties and regions of elevated pore-fluid pressure along subduction plate interfaces (e.g., Bilek et al., 2004; Kodaira et al., 2004; Kitajima and Saffer, 2012; Ikari et al., 2013). In these cases a large amount of energy is dissipated during deformation, making less energy available for seismic radiation (see Schwartz and Rokosky, 2007).

Depending on the dimensions and distributions of MTDs with respect to the thickness of a subduction plate interface and on the volume of host sediments, this structural heterogeneity may strongly control the seismic behavior, as discussed in the next section.

4.2. Dimensions of subducted MTDs and seismic behavior

Direct measurements of the thickness of subduction plate interfaces between zero and 15 km depths in modern and ancient convergent margins show that this boundary can be defined as an intensely sheared fault system, which is crosscut by sharp, discrete secondary faults within or along its edges (Rowe et al., 2013). The total thickness of a shear zone encompassing all simultaneously active fault strands and defining a subduction plate interface increases to 100‑350 m at 1‑2 km below seafloor, and this thickness is maintained down to a depth of ~15 km (Rowe et al., 2013). Incorporation of MTDs with different sizes (up to ≥1000 km^2) significantly affects the rheological heterogeneity and the mechanical anisotropy of the architecture of shallow subduction plate interfaces and may trammel their shear zone for an area up to thousands of square kilometers (Figs. 3A, 4B). The contrast between fluid-rich material supplied by MTDs and the surrounding drier and more lithified hosting sediments may create a complex patchiness across an subduction plate interface, implying deviation and concentration of fluids and shear with possible variation of mechanical intraplate coupling (e.g., Sage et al., 2006 and reference therein). This complex patchiness across the shallow subduction plate interface (Fig. 4B) is expected to show scale invariance with that observed at a mesoscale (compare Fig. 4A, B and C) within highly heterogeneous MTDs (see also Fagereng and Sibson, 2010 for tectonic mélanges). Thus, the contrast in permeability and lithification may be interpreted as patchiness of the material rheology (i.e., heterogeneous MTDs and homogeneous trench-fill sediments). As for a subduction plate interface weakened by the occurrence of several small "asperities" (see, e.g., Lay and Kanamori, 1981; Schwartz and Rokosky, 2007), the patchiness configuration may complicate the internal architecture of the seismogenic zone in different ways (Fig. 4B). This situation depends on the size and distribution of MTDs with respect to the volume and thickness of surrounding trench-fill sediments, and thus conditioning the seismic behavior. We describe below two end-members of patchiness configuration.
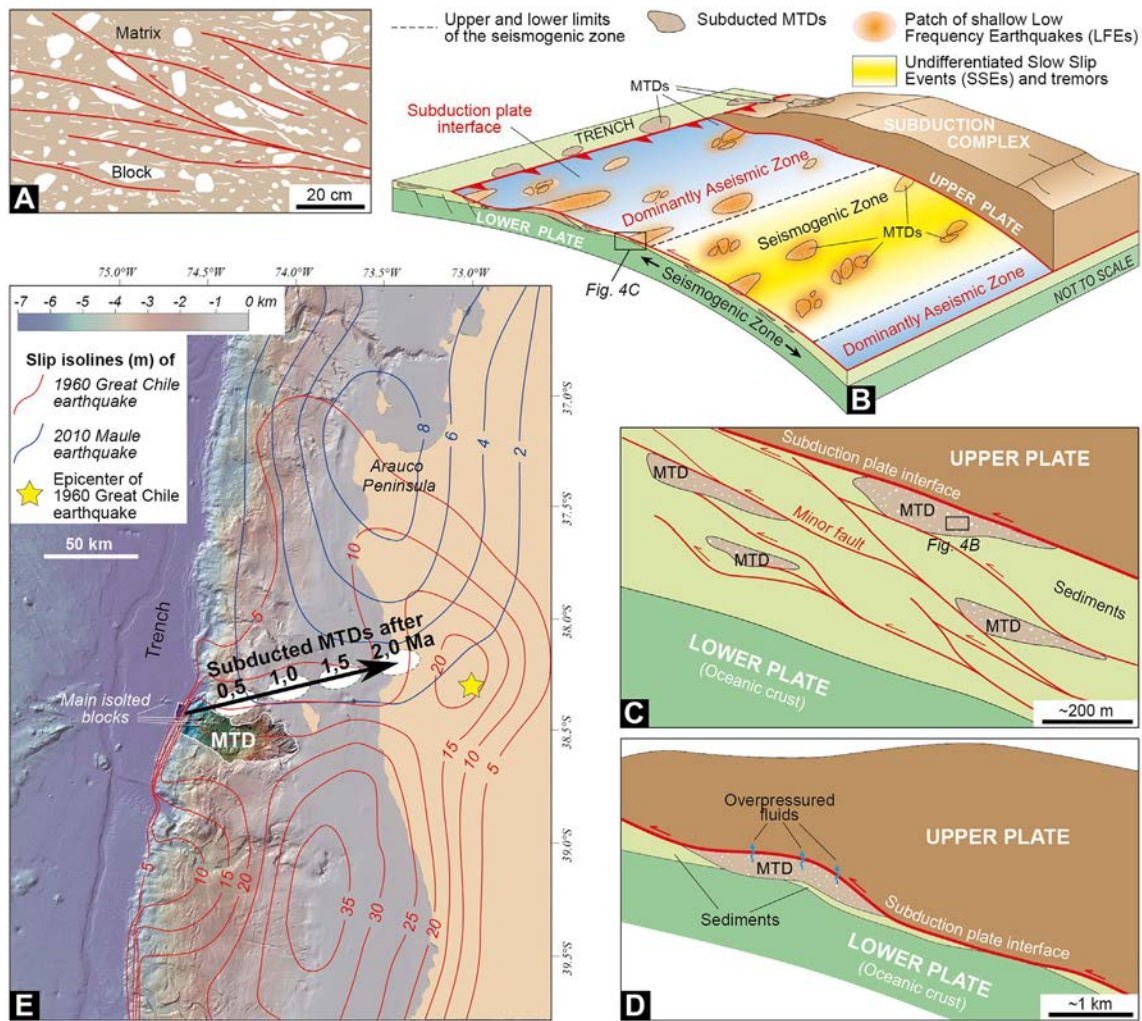
Fig. 4. (A) Internal mesoscale block-in-matrix fabric of an MTD subducted to the up-dip limit of a shallow seismogenic zone. Note the inferred strain partitioning along some anastomosing shear surfaces around blocks and clasts, causing limited interaction between them. This process facilitates their unstable sliding in a frictionally stable or conditionally stable matrix. (B) Schematic view of a subduction plate interface showing probable relationships between the distribution of subducted MTDs and SSEs. Location of SSEs modified from Obara and Kato (2016). (C) Scattered distribution of several small- to medium-size, fluid-rich MTDs in a subduction plate interface, dominated by dehydrated host sediments. This configuration promotes the formation of a heterogeneous fault network, which potentially leads into a spectrum of interconnected seismic behavior types ranging from interseismic locking to aseismic creep, and transition in between them. (D) Subduction of giant MTDs obstructing the subduction plate interface (SPI) triggers preferential concentration and compartmentalization of high- to over-pressured fluids (and related shear-weakening) and shearing at their boundaries. (E) Bathymetric map of the overlapping segments of the northern limit of the M_w 9.5 Great Chile and the M_w 8.8 Maule earthquake ruptures. Note the spatial relationships between the calculated positions of subducted MTDs (gray ellipses) and the slip distribution (from Moreno et al., 2009, 2012) of those earthquakes (modified from Geersen et al., 2013). Scarp embayment of the giant MTD (from Geersen et al., 2011) is outlined in white. Black arrow indicates the inferred position of the subducted, early-Middle Pleistocene MTDs, ~0 to 2 million years after their subduction started (plate dip angle = 25°, convergence rate = 6.6 cm·a^{-1}). Bathymetric data from GeoMapApp (http://www.geomapapp.org, see also Ryan et al., 2009).

Scattered distribution of several small to medium (10–1000 km^2) and fluid-rich MTDs in a dominant volume of dehydrated hosting sediments produces a patchiness configuration across the subduction plate interface (Fig. 4A, C) that favors the generation of anastomosing networks of linked fault-segments, which facilitate fluid migration and redistribution (e.g., Curewitz and Karson, 1997). This heterogeneous fault network is scale-invariant (compare Fig. 4A–C) as in the block-in-matrix fabric of MTDs and tectonic mélanges on land, and is closely related to stress cycles through the creation or reduction of permeability (Fisher et al., 1995; Sibson, 2013). Periodic slip along this heterogeneous fault network within the host sediments and cracking and sealing of microfractures within MTDs triggers a wide spectrum of interconnected seismic behaviors, ranging from inter-seismic locking to aseismic creep, and their mutual transition as documented at smaller scales from tectonic mélanges (see Fagereng and Sibson, 2010). The expected seismic behavior is comparable to that postulated for a subduction plate interface that is characterized by numerous small asperities where the stress increments communicated to adjacent zones are inadequate to cause

larger rupture propagation because of the relative small size of subducted asperities (e.g., Lay and Kanamori, 1981). Offshore of Southern Chile, seismic images show highly inhomogeneous structures of the underthrust section, which is characterized by a chaotic mixture of failed and slumped material that hampers the development of a continuous slip zone as required for large earthquake rupture propagation (Geersen et al., 2013). This phenomenon is well documented by the abrupt decrease of slip distribution of the ruptures associated with the M_w 9.5 Great Chile and M_w 8.8 Maule earthquakes in a domain corresponding to the inferred position of the Early to Middle Pleistocene heterogeneous MTDs, from 0 to 2 million years after their subduction started (Geersen et al., 2013; Fig. 4E).

On the contrary, a patchiness configuration characterized by the subduction of small- to medium-clustered or single giant MTDs (up to hundreds of meters thick and thousands of km^2 wide) creates an aberrance along subduction plate interfaces (Fig. 4D), and causes the concentration of over-pressurized fluids and shearing at their boundaries. This development results in significant mechanical weakening and

shear zone clustering. This phenomenon has been documented from the active continental margin of Ecuador where seismic images have shown that mechanical weakening and focused shearing concentrate above a large, low-viscosity and fluid-rich lens located at the bottom of the upper plate; this lens has been interpreted as a subducted MTD (Sage et al., 2006). Proportional to the dimensions of these giant MTDs, their larger size of the slip area with respect to those associated with scattered small- to medium MTDs may thus potentially favor higher magnitude earthquakes.

5. Concluding remarks

The internal architecture and mechanical properties of subducted material, the thickness of a subduction plate interface (or megathrust fault zone), the homogeneity versus heterogeneity of subducted sediments, and the spacing, distribution and size of "asperities" play a significant role in influencing the seismic behavior at shallow subduction plate interfaces. Our study shows that the subduction of medium to giant heterogeneous MTDs represents an additional factor in controlling seismic behavior by increasing the structural and compositional heterogeneity of subduction plate interfaces.

Heterogeneous fabric and composition of MTDs diminish the effectiveness of seismic ruptures significantly through the redistribution of overpressurized fluids and strain, and thereby favoring the occurrence of slow-slip events, very low frequency earthquakes, non-volcanic tremors, and creep, compared to regular earthquakes at least in shallow parts of a subduction plate interface. The large dimensions and distribution of medium ($10-1000\,km^2$) to giant ($\geq 1000\,km^2$), mud-rich heterogeneous MTDs in comparison to the average thickness of a subduction plate interface ($100-350\,m$ to a depth of ~15 km, see Rowe et al., 2013) and to the volume of hosting sediments (Fig. 4B) may also favor the concentration of both over-pressurized fluids and shearing. These features form a wide spectrum of single to interconnected faults with different lengths, leading to a wide range of interconnected seismic behaviors (Fig. 4A-D). Such seismic patterns are expected to show the same fault motion in the adjacent areas, ranging from stable sliding (i.e., steady aseismic creep) within MTDs (Fig. 4A, B) to fast rupture (i.e., stick-slip behavior) at boundaries between MTDs and host sediments or along décollement surfaces (Fig. 4B, C). These end members are commonly observed at the updip and downdip edges of seismogenic subduction plate interfaces, where episodic tremors and SSEs are geodetically and/or seismically identified. Transition in frictional properties from velocity weakening to velocity strengthening occurs in such interfaces. These seismic patterns also occur within seismogenic zones (e.g., Schwartz and Rokosky, 2007) and show complex temporal and spatial relationships with giant earthquake occurrences (Fig. 4B; Peng and Gomberg, 2010; Kato et al., 2012; Ito et al., 2013). One can infer the position of the subducted part of an MTD if the timing of its emplacement at a trench, the convergence rate of the downgoing slab, and the dip angle of this slab are known. Geersen et al. (2013) have shown that the positions of the subducted MTDs on the Nazca Plate (off the shore of southern Chile) correspond to the locations of the sharp terminations of the ruptures, which were associated with the 1960 Great Chile and the 2010 Maule giant earthquakes (Fig. 4E).

Making direct observations of the internal architecture of modern subduction plate interfaces is nearly impossible. Therefore, systematic studies of shear zones in exhumed analogues of modern MTDs in ancient subduction zone complexes are of paramount importance in better understanding the role of heterogeneity in controlling seismic rupture control at convergent margins.

References

Bilek, S.L., Lay, T., Ruff, L.J., 2004. Radiated seismic energy and earthquake source duration variations from teleseismic source time functions for shallow subduction zone thrust earthquakes. Journal of Geophysical Research 109:B09308. https://doi.org/10.1029/2004JB003039.

Bletery, Q., Thomas, A.M., Rempel, A.W., Karlstrom, L., Sladen, A., De Barros, L., 2016. Mega-earthquakes rupture flat megathrusts. Science 354, 1027-1031.

Brizzi, S., Sandri, L., Funiciello, F., Corbi, F., Piromallo, C., Heuret, A., 2018. Multivariate statistical analysis to investigate subduction zone parameters favoring the occurrence of great earthquakes. Tectonophysics 728:92-103. https://doi.org/10.1016/j.tecto.2018.01.027.

Byrne, D.E., Davis, D.M., Sykes, L.R., 1988. Loci and maximum size of thrust earthquakes and the mechanics of the shallow region of subduction zones. Tectonics 7, 833-857.

Camerlenghi, A., Pini, G.A., 2009. Mud volcanoes, olistostromes and Argille scagliose in the Mediterranean region. Sedimentology 56, 319-365.

Cardona, S., Wood, L.J., Day-Stirrat, R.J., Moscardelli, L., 2016. Fabric development and pore-throat reduction in a mass-transport deposit in the JUBILEE Gas Field, Eastern Gulf of Mexico: consequences for the Sealing Capacity of MTDs. In: Lamarche et al. (Ed.), Submarine Mass Movements and their Consequences: Advances in Natural and Technological Hazard Research. 41. Springer Science+Business Media B.V., pp. 27-37.

Clift, P., Vannucchi, P., 2004. Controls on tectonic accretion versus erosion in subduction zones: implications for the origin and recycling of the continental crust. Reviews of Geophysics 42:RG2001. https://doi.org/10.1029/2003RG000127.

Cloos, M., 1982. Flow melanges: numerical modeling and geologic constraints on their origin in the Franciscan subduction complex, California. Geological Society of America Bulletin 93, 330-345.

Codegone, G., Festa, A., Dilek, Y., 2012. Formation of Taconic Mélanges and broken formations in the Hamburg Klippe, Central Appalachian Orogenic Belt, eastern Pennsylvania. Tectonophysics 568-569, 215-229.

Coleman, J.M., Prior, D.B., 1988. Mass wasting on continental margins. Annual Review of Earth and Planetary Sciences 16, 101-119.

Collot, J.-Y., Lewis, K., Lamarche, G., Lallemand, S., 2001. The giant Ruatoria debris avalanche on the northern Hikurangi margin, New Zealand: result of oblique seamount subduction. Journal of Geophysical Research 106 (9), 19271-19297.

Corbi, F., Herrendörfer, R., Funiciello, F., van Dinther, Y., 2017. Controls of seismogenic zone width and subduction velocity on interpolate seismicity: insights from analog and numerical models. Geophysical Research Letters 44, 6082-6091.

Cowan, D.S., 1985. Structural styles in Mesozoic and Cenozoic mélanges in the western Cordillera of North America. Geological Society of America Bulletin 96, 451-462.

Curewitz, D., Karson, J.A., 1997. Structural settings of hydrothermal outflow: fracture permeability maintained by fault propagation and interaction. Journal of Volcanology and Geothermal Research 79 (3), 149-168.

Dielforder, A., Berger, A., Herwegh, M., 2016. The accretion of foreland basin sediments during early stages of continental collision in the European Alps and similarities to accretionary wedge tectonics. Tectonics 35 (10), 2216-2238.

Dilek, Y., Festa, A., Ogawa, Y., Pini, G.A., 2012. Chaos and geodynamics: mélanges, mélange-forming processes and their significance in the geological record. Tectonophysics 568-569, 1-6.

Doglioni, C., Carminati, E., Cuffaro, M., Scrocca, D., 2007. Subduction kinematics and dynamic constraints. Earth-Science Reviews 83, 125-175.

Fagereng, Å., 2011. Frequency-size distribution of competent lenses in a block-in-matrix mélange: imposed length scales of brittle deformation? Journal of Geophysical Research 116:B05302. https://doi.org/10.1029/2010JB007775.

Fagereng, Å., Sibson, R.H., 2010. Mélange rheology and seismic style. Geology 38, 751-754.

Fagereng, Å., Remitti, F., Sibson, R.H., 2011. Incrementally developed slickenfibers - geological record of repeating low stress-drop seismic events? Tectonophysics 510, 381-386.

Fagereng, Å., den Hartog, S.A.M., 2016. Subduction megathrust creep governed by pressure solution and frictional-viscous flow. Nature Geoscience 10:51-57. https://doi.org/10.1038/ngeo2857.

Festa, A., Pini, G.A., Dilek, Y., Codegone, G., 2010. Mélanges and mélange-forming processes: a historical overview and new concepts. In: Dilek, Y. (Ed.). Alpine Concept in GeologyInternational Geology Review 52 (10−12), 1040-1105.

Festa, A., Dilek, Y., Codegone, G., Cavagna, S., Pini, G.A., 2013. Structural anatomy of the Ligurian accretionary wedge (Monferrato, NW Italy), and evolution of superposed mélanges. Geological Society of America Bulletin 125 (9-10), 1580-1598.

Festa, A., Dilek, Y., Gawlick, H.-J., Missoni, S., 2014. Mass-transport deposits, olistostromes and soft-sediment deformation in modern and ancient continental margins, and associated natural hazards. Marine Geology 356 (Special Issue):1-4. https://doi.org/10.1016/j.margeo.2014.09.001.

Festa, A., Ogata, K., Pini, G.A., Dilek, Y., Codegone, G., 2015. Late Oligocene-early Miocene olistostromes (sedimentary mélanges) as tectono-stratigraphic constraints to the geodynamic evolution of the exhumed Ligurian accretionary complex (Northern Apennines, NW Italy). International Geology Review 57 (5-8), 540-562.

Festa, A., Ogata, K., Pini, G.A., Dilek, Y., Alonso, J.L., 2016. Origin and significance of olistostromes in the evolution of orogenic belts: a global synthesis. Gondwana Research 39, 180–203.

Fisher, D., Byrne, T., 1987. Structural evolution of underthrusted sediments, Kodiak Islands, Alaska. Tectonics 6 (6), 775–793.

Fisher, D.M., Brantley, S.L., Everett, M., Dzvonik, J., 1995. Cyclic fluid flow through a regionally extensive fracture network within the Kodiak accretionary prism. Journal of Geophysical Research 100 (B7), 12881–12894.

Geersen, J., Volker, D., Behrmann, J.H., Reichert, C., Krastel, S., 2011. Pleistocene giant slope failure offshore Arauco Peninsula, Southern Chile. Journal of the Geological Society, London 168, 1237–1248.

Geersen, J., Volker, D., Behrmann, J.H., Klaschen, J.H., Weinrebe, W., Krastel, S., Reichert, C., 2013. Seismic rupture during the 1960 Great Chile and the 2010 Maule earthquakes limited by a giant Pleistocene submarine slope failure. Terra Nova 25, 472–477.

Heuret, A., Conrad, C.P., Funiciello, F., Lallemand, S., Sandri, L., Heuret, A., Conrad, C.P., Funiciello, F., Lallemand, S., Sandri, L., 2012. Relation between subduction megathrust earthquakes, trench sediment thickness and upper plate strain. Geophysical Research Letters 39:L05304. https://doi.org/10.1029/2011GL050712.

Huene, R., Bourgois, J., Miller, J., Pautot, G., 1989. A large tsunamogenic landslide and debris flow along the Peru Trench. Journal of Geophysical Research 94 (B2):1703–1714. https://doi.org/10.1029/JB094iB02p01703.

Ide, S., Beroza, G.C., Shelly, D.R., Uchide, T., 2007. A scaling law for slow earthquakes. Nature 447, 76–79.

Ikari, M.J., Marone, C., Saffer, D.M., Kopf, A.J., 2013. Slip weakening as a mechanism for slow earthquakes. Nature Geoscience 6, 468–472.

Ito, Y., Hino, R., Kido, M., Fujimoto, H., Osada, Y., Inazu, D., Ohta, Y., Iinuma, T., Ohzono, M., Miua, S., Mishina, M., Suzuki, K., Tsuji, T., Ashi, J., 2013. Episodic slow slip events in the Japan subduction zone before the 2011 Tohoku-Oki earthquake. Tectonophysics 600, 14–26.

Kato, A., Obara, K., Igarashi, T., Tsuruoka, H., Nakagawa, S., Hirata, N., 2012. Propagation of slow slip leading up to the 2011 Mw 9.0 Tohoku-Oki earthquake. Science 335, 705–708.

Kelleher, J., Savino, J., Rowlett, H., McCann, W., 1974. Why and where great thrust earthquakes occur along island arcs. Journal of Geophysical Research 79, 4.889–4899.

Kimura, G., Yamaguchi, A., Hojo, M., Kitamura, Y., Kameda, J., Ujiie, K., Hamada, Y., Hamahasi, M., Hina, S., 2012. Tectonic mélange as fault rock of subduction plate boundary. Tectonophysics 568–569, 25–38.

Kitajima, H., Saffer, D.M., 2012. Elevated pore pressure and anomalously low stress in regions of low frequency earthquakes along the Nankai subduction megathrust. Geophysical Research Letters 39, L23301.

Kodaira, S., Iidaka, T., Kato, A., Park, J., Iwasaki, T., Kaneda, Y., 2004. High pore fluid pressure may cause silent slip in the Nankai Trough. Science 304, 1295–1299.

Kopp, H., 2013. The control of subduction zone structural complexity and geometry on margin segmentation and seismicity. Tectonophysics 589, 1–16.

Lamarche, G., Joanne, C., Collot, J.-Y., 2008. Successive, large mass-transport deposits in the south Kermadec fore-arc basin, New Zealand: the Matakaoa Submarine Instability Complex. Geochemistry, Geophysics, Geosystems 9 (4):Q04001. https://doi.org/10.1029/2007GC001843.

Lay, T., Kanamori, H., 1981. An asperity model of large earthquake sequences. In: Simpson, D.W., Richards, P.G. (Eds.), Earthquake Prediction, an International Review. American Geophyisical Union, Washington, D.C., pp. 579–592 Ed.

Lewis, K.B., Lallemand, S., Carter, L., 2004. Collapse in a Quaternary shelf basin off East Cape, NewZealand: evidence for the passage of a subducted seamount inboard of the Ruatoria giant avalanche. New Zealand Journal of Geology and Geophysics 47, 415–429.

Lucente, C.C., Pini, G.A., 2003. Anatomy and emplacement mechanism of a large submarine slide within the Miocene foredeep in the Northern Apennines, Italy: a field perspective. American Journal of Science 303, 565–602.

McAdoo, B.G., Pratson, L.F., Orange, D.L., 2000. Submarine landslide geomorphology, US continental slope. Marine Geology 169, 103–136.

Mittempergher, S., Cerchiari, A., Remitti, F., Festa, A., 2017. From soft sediment deformation to fluid assisted faulting in the shallow part of a subduction megathrust analogue: the Sestola Vidiciatico tectonic unit (Northern Apennines, Italy). Geological Magazine (Online First View). https://doi.org/10.1017/S0016756817000668.

Mohrig, D., Whipple, K.X., Hondzo, M., Ellis, C., Parker, G., 1998. Hydroplaning of subaqueous debris flows. Geological Society of America Bulletin 110, 387–394.

Moreno, M.S., Bolte, J., Klotz, J., Melnick, D., 2009. Impact of megathrust geometry on inversion of coseismic slip from geodetic data: application to the 1960 Chile earthquake. Geophysical Research Letters 36:L16310. https://doi.org/10.1029/2009GL039276.

Moreno, M.S., Meknick, D., Rosenau, M., Baez, J., Klotz, J., Oncken, O., Tassara, A., Chen, J., Bataille, K., Bevis, M., Socquet, A., Bolte, J., Vigny, C., Brooks, B., Rayder, I., Grund, V., Smalley, B., Carizzo, D., Bartsch, M., Hase, H., 2012. Toward understanding tectonic control on the Mw 8.8 2010 Maule Chile earthquake. Earth and Planetary Science Letters 321-322, 152–160.

Moscardelli, L., Woods, L., 2008. A new classification system for mass transport complexes in offshore Trinidad. Basin Research 20, 73–98.

Moscardelli, L., Woods, L., 2016. Morphometry of mass-transport deposits as a predictive tool. Geological Society of America Bulletin 128 (1–2), 47–80.

Mutti, E., Carminatti, M., Moreira, J.L.P., Grassi, A.A., 2006. Chaotic deposits: examples from the Brazilian offshore and, from outcrop studies in the Spanish Pyrenees and Northern Apennines, Italy. American Association Petroleum Geologists Annual Meeting, April 9–12, Houston, Texas.

Obara, K., Kato, A., 2016. Connecting slow earthquakes to huge earthquakes. Science 353 (6296), 253–257.

Ogata, K., Mountjoy, JJ., Pini, G.A., Festa, A., Tinterri, E., 2014a. Shear zone liquefaction in mass transport deposit emplacement: a multi-scale integration of seismic reflection and outcrop data. Marine Geology 356 (Special Issue), 50–64.

Ogata, K., Pogačnik, Ž., Pini, G.A., Tunis, G., Festa, A., Camerlenghi, A., Rebesco, M., 2014b. The carbonate mass transport deposits of the Paleogene Julian-Slovenian Basin (Italy/Slovenia): internal anatomy and inferred genetic processes. Marine Geology 356, 88–110.

Ortiz-Karpf, A., Hodgson, D.M., Jackson, C.A.-L., McCaffrey, W.D., 2016. Mass-transport complexes as markers of deep-water fold-and-thrust belt evolution: insights from the southern Magdalena Fan, offshore Colombia. Basin Research (Online First View):1–24. https://doi.org/10.1111/bre.12208.

Peng, Z., Gomberg, J., 2010. An intergrated perspective of the continuum between earthquakes and slow-slip phenomena. Nature Geoscience 3, 599–607.

Peterson, E.T., Seno, T., 1984. Factors affecting seismic moment release rates in subduction zones. Journal of Geophysical Research 89 (B12), 10.233–10.248.

Pini, G.A., 1999. Tectonosomes and olistostromes in the Argille Scagliose of the Northern Apennines, Italy. Geological Society of America Special Papers 335, 73.

Pini, G.A., Ogata, K., Camerlenghi, A., Festa, A., Lucente, C.C., Codegone, G., 2012. Sedimentary mélanges and fossil mass-transport complexes: a key for better understanding submarine mass movements? In: Yamada, Y. (Ed.), Submarine Mass Movements and Their Consequences. Advances in Natural and Technological Hazards Research 31. Springer Science+Business Media B.V., pp. 585–594

Platt, J.P., 2015. Origin of Franciscan blueschist-bearing mélange at San Simeon, central California coast. International Geology Review 57 (5–8), 843–868.

Ratzov, G., Collot, J.-Y., Sosson, M., Migeon, S., 2010. Mass-transport deposits in the northern Ecuador subduction trench: result of frontal erosion over multiple seismic cycles. Earth and Planetary Science Letters 296, 89–102.

Raymond, L.A., 1984. Classification of melanges. In: Raymond, L.A. (Ed.), Melanges: their nature, origin and significance. Boulder, Colorado. Geological Society of America Special Papers 198, 7–20.

Rowe, C.D., Moore, J.C., Remitti, F., the IODP Expedition 343 Science Party, 2013. The thickness of subduction plate boundary faults from the seafloor into the seismogenic zone. Geology 41 (9), 991–994.

Ruff, L.J., 1989. Do trench sediments affect great earthquake occurrence in subduction zones. Pure and Applied Geophysics 129, 263–282.

Ryan, W.B.F., Carbotte, S.M., Coplan, J.O., O'Hara, S., Melkonian, A., Arko, R., Weissel, R.A., Ferrini, V., Goodwillie, A., Nitsche, F., Bonczkowski, J., Zemsky, R., 2009. Global multi-resolution topography synthesis. Geochemistry Geophysics Geosystems 10: Q03014. https://doi.org/10.1029/2008GC002332.

Sage, F., Collot, J.-Y., Ranero, C.R., 2006. Interplate patchiness and subduction-erosion mechanisms: evidence from depth-migrated seismic images at the Central Ecuador convergent margin. Geology 34 (12), 997–1000.

Sawyer, D.E., Flemings, P.B., Dugan, B., Germaine, J.T., 2009. Retrogressive failures recorded in mass transport deposits in the Ursa Basin, Northern Gulf of Mexico. Journal of Geophysical Research 114:B10102. https://doi.org/10.1029/2008JB006159.

Schellart, W.P., Rawlinson, N., 2013. Global correlations between maximum magnitudes of subduction zone interface thrust earthquakes and physical parameters of subduction zones. Physics of the Earth and Planetary Interiors 225, 41–67.

Scholl, D.W., von Huene, R., 2009. Implications of estimated magmatic additions and recycling losses at the subduction zones of accretionary (non-collisional) and collisional (suturing) orogens. In Cawood, P.A., Kroner, A. (Eds.), Earth accretionary systems in space and time. The Geological Society, London, Special Publications 318, 105–125.

Scholl, D.W., Kirby, S.H., von Huene, R., Ryan, H., Wells, R.E., Geist, E.L., 2015. Great (≥Mw8.0) megathrust earthquakes and the subduction of excess sediment and bathymetrically smooth seafloor. Geosphere 11 (2), 236–265.

Scholz, C.H., 2002. The Mechanics of Earthquakes and Faulting. Cambridge Univ. Press, Cambridge, UK, p. 429.

Scholz, C.H., Campos, J., 1995. On the mechanism of seismic decoupling and back-arc spreading in subduction zones. Journal of Geophysical Research 100, 901–909.

Scholz, C.H., Campos, J., 2012. The seismic coupling of subduction zones revisited. Journal of Geophysical Research 117:B05310. https://doi.org/10.1029/2011JB009003.

Schwartz, S.Y., Rokosky, J.M., 2007. Slow slip event and seismic tremor at circum-Pacific subduction zones. Reviews of Geophysics 45:RG3004. https://doi.org/10.1029/2006RG000208.

Seno, T., 2017. Subducted sediment thickness and Mw9 earthquakes. Journal of Geophysical Research: Solid Earth 122, 470–491.

Sibson, R.H., 2013. Stress switching in subduction forearcs: implications for overpressure containment and strength cycling on megathrusts. Tectonophysics 600, 142–152.

Skempton, A.W., 1970. First-time slides in over-consolidated clays. Géotechnique, London, England 20 (3), 320–324.

Strasser, M., Kölling, M., dos Santos Ferreira, C., Fink, H.G., Fujiwara, T, Henkel, S., Ikehara, K., Kanamatsu, T., Kawamura, K., Kodaira, S., Römer, M., Wefer, G., the R/V Sonne Cruise SO219A and JAMSTEC Cruise MR12-E01 scientists, 2013. A slump in the trench: tracking the impact of the 2011 Tohoku-Oki earthquake. Geology 41 (8), 935–938.

Urgeles, R., Camerlenghi, A., 2013. Submarine landslides of the Mediterranean Sea: triggering mechanisms, dynamics, and frequency-magnitude distribution. Journal of Geophysical Research - Earth Surface 118, 2600–2618.

Uyeda, S., Kanamori, H., 1979. Back-arc opening and the mode of subduction. Journal of Geophysical Research 84, 1049–1061.

Vannucchi, P., Remitti, F., Bettelli, G., 2008. Geological record of fluid flow and seismogenesis along an erosive subducting plate boundary. Nature 451, 699–703.

Vannucchi, P., Sage, F., Phipps Morgan, J., Remitti, F., Collot, J.-Y., 2012. Toward a dynamic concept of the subduction channel at erosive convergent margins with implications for interplate material transfer. Geochemistry, Geophysics, Geosystems 13:Q02003. https://doi.org/10.1029/2011GC003846.

von Huene, R., Ranero, C.R., Vannucchi, P., 2004. Generic model of subduction erosion. Geology 32, 913–916.

Woodcock, N.H., 1979. The use of slump structures as palaeoslope orientation estimators. Sedimentology 26 (1), 83–99.